O@PoC
eISSN 2399-3685

Ophthalmol @ Point Care 2017; 1(1): e36-e44
DOI: 10.5301/oapoc.0000009

RESEARCH @ POINT OF CARE

Open Access

Integrated imaging of avascular serous pigment epithelium detachment in age-related macular degeneration

Giuseppe Querques[1,2], Marco R. Pastore[1,3], Houda Khlifi[2], Anouk Georges[2], Lea Querques[3], Eric H. Souied[1]

[1] Department of Ophthalmology, Centre Hospitalier Intercommunal de Creteil University Paris Est Creteil, Creteil - France
[2] Department of Ophthalmology, University Vita-Salute, IRCCS Ospedale San Raffaele, Milano - Italy
[3] University Eye Clinic of Trieste, Ospedale Maggiore, Trieste - Italy

ABSTRACT

Introduction: This study describes the imaging of avascular serous pigment epithelial detachment (PED) in age-related macular degeneration (AMD) patients using confocal scanning laser ophthalmoscopy and spectral-domain optical coherence tomography (SD-OCT).

Methods: A total of 18 patients with avascular serous PED underwent assessment of best-corrected visual acuity, infrared (IR) reflectance, fundus autofluorescence (FAF), fluorescein angiography (FA), indocyanine green angiography (ICGA), and SD-OCT evaluation at baseline and at last follow-up visit. The imaging of avascular PED was compared with vascularized PED.

Results: A total of 23 eyes with 15.5 ± 6.4 months' follow-up were included. Imaging revealed 3 features associated with avascular serous PED. A reticular pattern, highly reflective (IR), and hyperautofluorescent matching with a reticular area of decreased fluorescence (FA and ICGA) was constantly observed (23/23 eyes). This reticular pattern correlated on SD-OCT with dense hypereflective deposits beneath and within the sensory retina. This reticular pattern was observed in only 2/19 eyes with vascular serous PED ($p<0.05$). A sharp border of increased IR reflectance, matching with a halo of reduced fluorescence on both FAF and late FA frames, was observed in 23/23 eyes. This sharp border appeared as a sharp hypofluorescent border on late ICGA frames, and as an abrupt elevation of the retinal pigment epithelium on SD-OCT. Hyporeflective fluid beneath the foveal depression was observed in 17/23 (74%) eyes. Only 1/23 eyes developed choroidal neovascularization during the follow-up.

Conclusions: Integrated imaging shows peculiar features of avascular PED and possibly contributes to distinguishing this clinical identity from neovascular AMD.

Keywords: Autofluorescence, Fluorescein angiography, Indocyanine green angiography, Infrared reflectance, Pigment epithelium detachment, Spectral domain optical coherence tomography

Introduction

Age-related macular degeneration (AMD) represents the leading cause of irreversible blindness in developed countries (1, 2). Exudative AMD is characterized by choroidal neovascularization (CNV) growth under the retinal pigment epithelium (RPE) with subsequent hemorrhage, pigment epithelial detachment (PED), exudative retinal detachment, disciform scarring, and retinal atrophy. The pathogenesis of PED in AMD is probably a continuum with that of degenerative changes occurring with age in Bruch's membrane and formation of CNV. PEDs in AMD are usually classified as serous PED, fibrovascular PED, and drusenoid PED (3).

Serous PED may occur with (vascularized PED) or, rarely, without CNV (nonvascularized PED, also called avascular PED). Vascularized serous PED was defined by Yannuzzi et al (4) on the basis of a hyperfluorescent area in the early phases of indocyanine green angiography ICGA with leakage in the late phase. Most of the serous PED are vascularized. ICGA imaging revealed that CNV is observed in 96% of patients with serous PED (5). The remaining 4% of eyes in this study had no evidence of underlying CNV on ICGA (avascular serous PED). The precise differences between these 2 clinical entities (vascular and avascular PED) are not completely understood. To date,

Accepted: April 17, 2017
Published online: May 10, 2017

Corresponding author:
Eric H. Souied
Department of Ophthalmology
University Paris 12
Henri Mondor Centre Hospitalier Intercommunal de Creteil
40 Avenue de Verdun
94000 Creteil, France
esouied@hotmail.com

there are still questions of whether avascular serous PED should be considered as a well-distinguished rare clinical entity, or as a form of occult CNV with PED in AMD that does not show signs of progression. Recently, intravitreal ranibizumab has been prospectively performed in a series of avascular PED (6). Over the 1 year study follow-up, the treatment was ineffective for improving retinal function, which was measured with best-corrected visual acuity (BCVA) and microperimetry. It supports the hypothesis that avascular serous PED is a subgroup of AMD distinct from vascularized serous PED.

Spectral-domain optical coherence tomography (SD-OCT) technology improves resolution, compared to previous time-domain OCT. Spectralis high-resolution SD-OCT (Spectralis SD-OCT, Heidelberg Engineering) is a high-speed OCT system (up to 40,000 axial scans per second) using spectral/Fourier domain detection, with an axial image resolution of 7 µm. Moreover, Spectralis SD-OCT, using confocal scanning laser ophthalmoscopy (cSLO) technology to track the eye and guide OCT to the selected location, gives a real-time reference for registration of the SD-OCT scan. Hence, by combining an angiograph (Heidelberg Retina Angiograph [HRA], Heidelberg Engineering, Heidelberg, Germany) with an OCT in Spectralis SD-OCT, an analysis of integrated fundus imaging including infrared (IR) reflectance, fundus autofluorescence (FAF) fluorescein angiographic (FA) and ICGA of lesions by cSLO technology and corresponding SD-OCT is possible.

In this study, our purpose was to analyze the integrated cSLO fundus imaging of AMD patients with avascular (nonvascularized) serous PED and, using real-time eye tracking technology, the corresponding high-resolution SD-OCT B-scan features.

Methods

We analyzed all consecutive AMD patients with avascular serous PED that presented at the University Eye Clinic of Creteil between January 2008 and January 2010. Criteria for diagnosis of avascular PEDs were hyperfluorescent PED on FA, and absence of hyperfluorescent lesions on early and late phases of ICGA in at least 2 consecutive follow-up visits (minimum 3-month intervals). In addition, in order to be included, all eyes had to show an absence of any characteristic signs of CNV, retinal angiomatous proliferation, or polypoidal choroid vasculopathy on FA and ICGA. Eyes with the appearance of a "notch" in serous PED were also excluded. Because the scanning laser ophthalmoscopy with integrated simultaneous indocyanine green (SLO-ICG) is a confocal technique, we adjusted the focus several times for each image. Several slices were explored until we could see any evidence of hyperfluorescence on late phases of ICG. Moreover, owing to the indistinct transition between large confluent drusen and avascular PED, these PEDs were defined as being >500 µm in diameter. Exclusion criteria were signs of any other retinal disease in the study eye, such as pattern dystrophy, and retinal vascular (i.e., diabetic retinopathy, and retinal vein occlusion), or vitreo-retinal diseases (i.e., vitreo-macular traction syndrome and epiretinal membrane).

Informed consent was obtained, as required by the French Bioethical Legislation, in agreement with the Declaration of Helsinki for research involving human subjects. The University Paris XII Institutional Review Board approval was obtained for this study.

All patients underwent a complete ophthalmologic examination, including assessment of BCVA, which was measured at 4 m with standard Early Treatment for Diabetic Retinopathy Study (ETDRS) charts, and HRA cSLO imaging (IR reflectance, FAF, FA, and ICGA) and tracked Spectralis SD-OCT. All cSLO images and SD-OCT scans were acquired by 2 of the authors (G.Q. and E.H.S.). Looking for possible CNVs, different planes of each avascular PED were analyzed by adequately adjusting the HRA cSLO focus, during both the FA and the ICGA examinations. Images prospectively collected were then evaluated regarding IR, FAF, FA, and ICGA findings, and the corresponding eye-tracked tomographic characteristics.

The Spectralis high resolution SD-OCT system provides in vivo details of the anatomy of the retina that nearly resembles histologic specimens (axial image resolution of 7 µm). Multiple single and/or a raster sets (field size 30 × 30 degrees; frequency of image acquisition up to 9 images/second) of high resolution B-scans were used to image the avascular PEDs. Using cSLO technology to track the eye, the OCT scans were guided from the retinal abnormalities associated with avascular PEDs as visualized on IR, FAF, FA, and ICGA frames; thus, the different cSLO images were used as a real-time reference for registration of the SD-OCT scan. SD-OCT scans were proportionally magnified for better visualization of retinal changes. The layers structure observed in proportionally magnified OCT images were described, analyzed, and interpreted by 2 senior retinal physicians (G.Q. and E.H.S.).

As part of this study, we also investigated the differences between avascular and vascular PED by analyzing the integrated cSLO fundus imaging and corresponding high-resolution SD-OCT B-scan features of a homogeneous population of exudative AMD patients with PED and occult CNV.

Statistical calculations were performed using SPSS software version 15.0 for Windows (SPSS). Comparisons of BCVA (converted to the logarithm of the minimum angle of resolution [LogMAR]) were performed using the Wilcoxon test (1 eye of each patient showing avascular PED at baseline was randomly selected). The chosen level of statistical significance was $p<0.05$.

Results

Patient demographics and macular characteristics of avascular serous PED

A homogeneous series of 23/36 eyes with avascular serous PED from 18 consecutive patients (5 males and 13 females; mean age 69.5 ± 7.2 years, range 58-82 years) were included for analysis (Tab. I). Baseline BCVA for avascular serous PED eyes ranged from 20/20 to 20/80, with a mean of 20/40 (0.31 ± 0.24 LogMAR); mean BCVA at last follow-up visit was 20/50 (0.42 ± 0.24 LogMAR; $p<0.05$). Mean follow-up was 15.5 ± 6.4 months. At baseline, the 9 fellow eyes of patients with avascular PED were diagnosed with either geographic atrophy (GA), or vascular PED, or CNV, or drusen (1, 1, 2, and 9 eyes, respectively). In only 1/23 eyes, CNV developed 12 months after the diagnosis of avascular PED, and BCVA dropped from

TABLE I - Patient demographics and macular characteristics

	Age (years)	Gender	Eye	BCVA baseline	BCVA Last follow-up	Diagnosis	Follow-up (months)	Time to CNV (months)
Patient 1	75	F	RE	20/20	20/40	aPED	24	
			LE	20/25	20/80	vPED		
Patient 2	60	F	RE	20/20	20/80	aPED	24	12
			LE	20/400	20/400	Occult CNV		
Patient 3	77	M	RE	20/25	20/25	aPED	9	
			LE	20/25	20/25	aPED		
Patient 4	61	M	RE	20/25	20/25	drusen	9	
			LE	20/50	20/50	aPED		
Patient 5	65	F	RE	20/20	20/20	Drusen	9	
			LE	20/80	20/80	aPED		
Patient 6	62	M	RE	20/20	20/20	aPED	9	
			LE	20/32	20/32	aPED		
Patient 7	75	F	RE	20/25	20/25	aPED	15	
			LE	20/32	20/32	aPED		
Patient 8	77	F	RE	20/80	20/125	aPED	24	
			LE	20/20	20/20	Drusen		
Patient 9	58	F	RE	20/20	20/32	aPED	24	
			LE	20/50	20/80	aPED		
Patient 10	76	F	RE	20/400	20/400	Occult CNV	24	
			LE	20/80	20/100	aPED		
Patient 11	74	F	RE	20/50	20/64	aPED	18	
			LE	20/32	20/32	Drusen		
Patient 12	82	F	RE	20/50	20/50	aPED	24	
			LE	20/32	20/40	Drusen		
Patient 13	73	M	RE	20/25	20/25	aPED	9	
			LE	20/25	20/25	aPED		
Patient 14	63	F	RE	20/320	20/320	GA	14	
			LE	20/50	20/50	aPED		
Patient 15	65	M	RE	20/64	20/64	Drusen	18	
			LE	20/80	20/80	aPED		
Patient 16	73	F	RE	20/80	20/100	aPED	12	
			LE	20/40	20/50	Drusen		
Patient 17	67	F	RE	20/64	20/80	aPED	12	
			LE	20/40	20/40	Drusen		
Patient 18	71	F	RE	20/32	20/80	aPED	12	
			LE	20/32	20/64	Drusen		

aPED = vascular pigment epithelium detachment; BCVA = best-corrected visual acuity; CNV = choroidal neovascularization; F = female; GA = geographic atrophy; LE = left eye; M = male; RE = right eye; vPED = vascular pigment epithelium detachment.

20/20 to 20/80. In all other included eyes (22/23 eyes) the final diagnosis at last follow-up visit remained avascular serous PED. In a few eyes, there was an increase in the height of the serous PED.

Specific cSLO-imaging features of avascular serous PED

On IR reflectance of the fundus, the avascular serous PED appeared as a dark area of inhomogeneous decreased IR

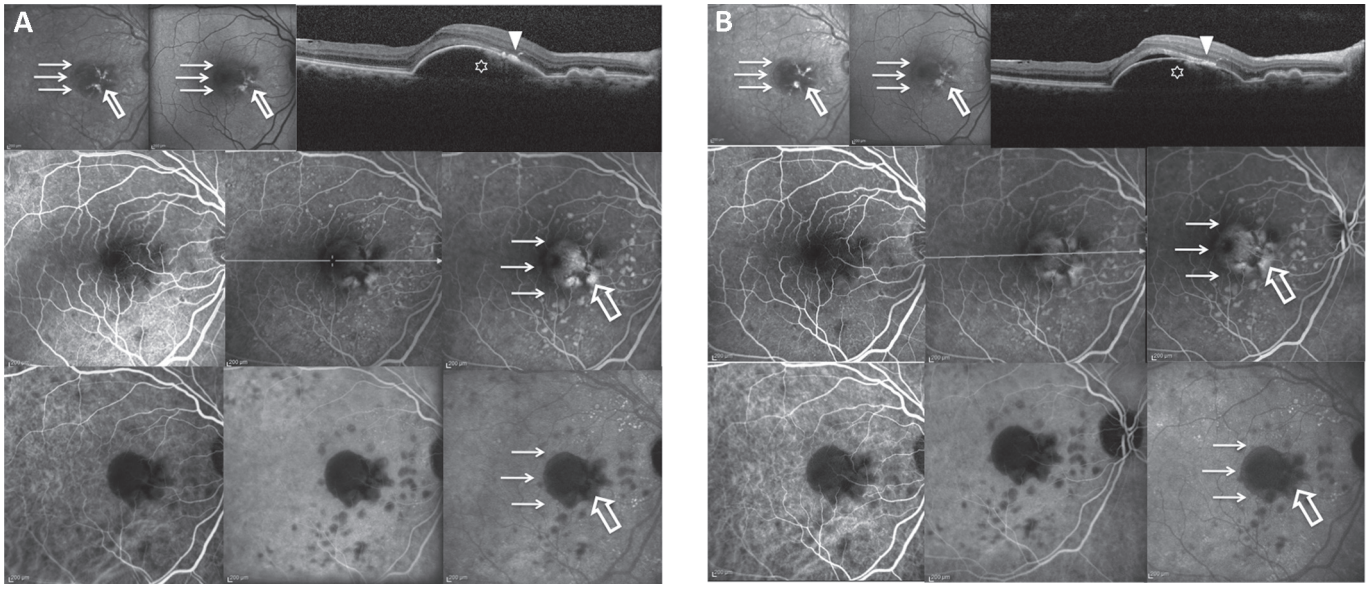

Fig. 1 - Imaging of avascular pigment epithelium detachment (PED). Patient 11, right eye, at baseline examination (**A**) and after 18 months (**B**). The infrared (IR) reflectance frame of the fundus (upper left panel), showing the avascular PED as a dark area of inhomogeneous decreased IR reflectance, is surrounded by a sharp border of increased IR reflectance (arrows). The dark area of inhomogeneous decreased IR reflectance matches with the area of inhomogeneous increased fluorescence as visualized on the fundus auto-fluorescence (FAF) (upper central panel) and the late fluorescein angiography (FA) frames (middle right panel). (Of note, a portion of the increased autofluorescence on the FAF image matches with some of the brighter areas on the IR image. The early and mid-FA frames are displayed on the middle left and middle central panels, respectively.) This area appears as hypofluorescent on the late indocyanine angiography (ICGA) frames (bottom right panel; the early and mid-ICGA frames are displayed on the bottom left and bottom central panels, respectively). The sharp border of increased IR reflectance (upper left panel, arrows), surrounding the avascular PED matches with the halo of reduced fluorescence on FAF (upper central panel, arrows) and the late FA frames (middle right panel, arrows), and with the sharp hypofluorescent border on the late ICGA frames (bottom right panel, arrows). Spectral-domain optical coherence tomography (SD-OCT) scan (upper right panel) shows mainly hyporeflective material consistent with serous accumulation of the avascular PED, with some collections of hypereflective material within the PED (asterisk). Here, we can also observe subretinal hyporeflective fluid under the fovea. On SD-OCT scan, an abrupt elevation of the retinal pigment epithelium is the characteristic associated with the well-defined border of the avascular PED. A highly reflective IR (upper left panel, open arrow) and hyperautofluorescent lesion (upper middle panel, open arrow) disposed in a reticular pattern matches with the reticular area of decreased fluorescence on the late FA (middle right panel, open arrow) and ICGA (bottom right panel, open arrow) frames. The material accumulated in these reticular lesions is responsible for the dense hypereflective deposits seen beneath and within the sensory retina on SD-OCT scan (upper right panel, arrowhead), which is associated with subretinal fluid to some extent.

reflectance, surrounded by a sharp border of increased IR reflectance (Figs. 1-4). In all eyes, an increased IR reflectance, presenting a reticular pattern, was detected within the dark area of inhomogeneous decreased IR reflectance (Figs. 1-4). The sharp border of increased IR reflectance was no longer visible once a CNV developed in one eye; thus, avascular serous PED turned into vascular PED (Fig. 4).

On FAF frames, the avascular serous PED appeared as an area of inhomogeneous mildly increased autofluorescence surrounded by a faint halo of reduced FAF (Figs. 1, 2). Furthermore, a highly hyperautofluorescent lesion disposed in a reticular pattern was clearly distinguished within the area of the avascular serous PED (Figs. 1, 2).

On late FA frames, the avascular serous PED appeared as a bright area of inhomogeneous increased fluorescence, surrounded by a halo of reduced fluorescence (Figs. 1-4). A hypofluorescent lesion, disposed in a reticular pattern, was detected within the area of inhomogeneous increased fluorescence on early phases (Figs. 1-4). Of note, once a CNV developed in 1 study eye, and avascular PED turned into vascular PED (Fig. 4), the halo of reduced fluorescence was replaced by a hyperfluorescent halo.

On late ICGA frames, the avascular serous PED appeared as a well-defined dark area of inhomogeneous decreased fluorescence with sharp borders (Figs. 1-4). A black hypofluorescent lesion disposed in a reticular pattern was faintly detected within the dark area of inhomogeneous decreased fluorescence (Figs. 1-4). Of note, once a CNV developed in 1 study eye, the PED still appeared as a dark area of inhomogeneous decreased fluorescence, even though the sharp borders disappeared (probably due to the fluid accumulation and leakage from the CNV) (Fig. 4).

cSLO tracked high-resolution SD-OCT features of avascular serous PED

On SD-OCT scans, the avascular serous PED was filled with hyporeflective fluid (Figs. 1-4). Collections of dense hypereflective material were seen over the RPE layer (Figs. 1-4). Some extent of hyporeflective fluid beneath the foveal depression was seen in 17/23 (74%) eyes (Figs. 1B, 4A). This hyporeflective fluid beneath the foveal depression was associated with collections of dense hypereflective material over the RPE layer. This hyporeflective fluid was not associated with progression

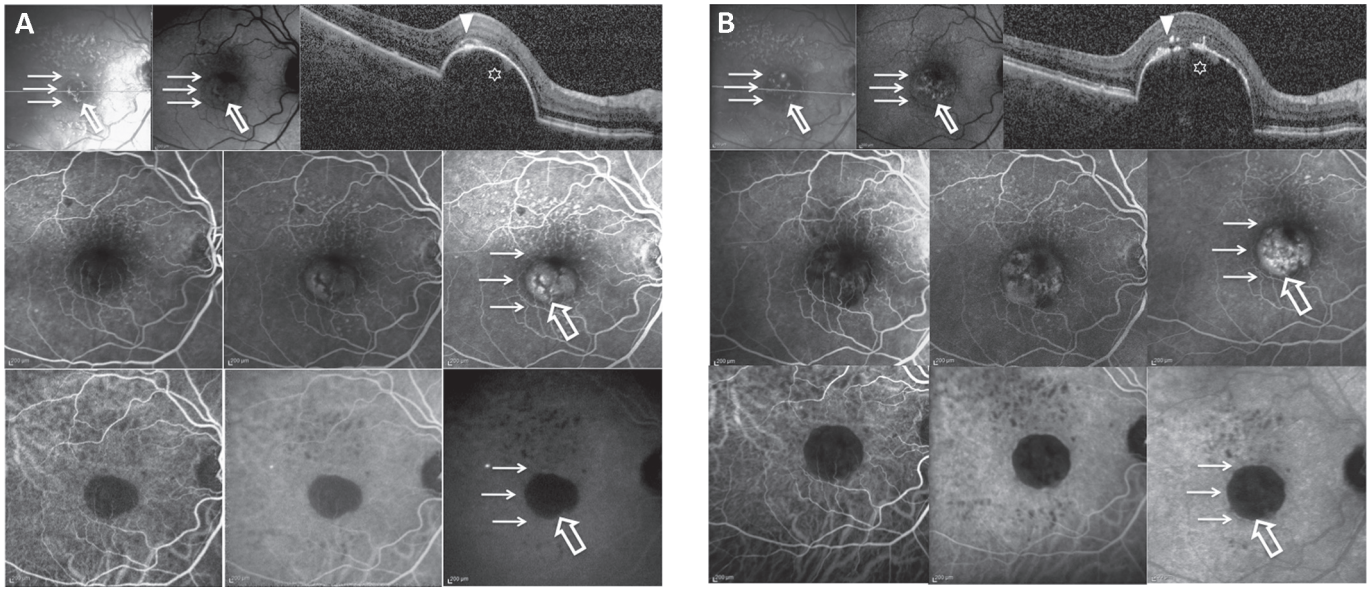

Fig. 2 - Follow-up of avascular pigment epithelium detachment (PED). Patient 12, right eye, at baseline examination (**A**) and after 24 months (**B**). The infrared (IR) reflectance frame of the fundus (upper left panel), showing the avascular PED as a dark area of inhomogeneous decreased IR reflectance, is surrounded by a sharp border of increased IR reflectance (arrows). The dark area of inhomogeneous decreased IR reflectance matches with the area of inhomogeneous increased fluorescence as visualized on the fundus auto-fluorescence (FAF) (upper central panel) and the late fluorescein angiography (FA) frames (middle right panel). (Of note, a portion of the increased autofluorescence on the FAF image matches with some of the brighter areas on the IR image. The early and mid-FA frames are displayed on the middle left and middle central panels, respectively). This area appears as hypofluorescent on the late indocyanine angiography (ICGA) frames (bottom right panel; the early and mid-ICGA frames are displayed on the bottom left and bottom central panels, respectively). The sharp border of increased IR reflectance (upper left panel, arrows), surrounding the avascular PED matches with the halo of reduced fluorescence on FAF (upper central panel, arrows) and the late FA frames (middle central panel, arrows), and with the sharp hypofluorescent border on the late ICGA frames (bottom right panel, arrows). Spectral-domain optical coherence tomography (SD-OCT) scan (upper right panel) shows mainly hyporeflective material consistent with serous accumulation of the avascular PED, with some collections of hypereflective material within the PED (asterisk). On SD-OCT scan, an abrupt elevation of the retinal pigment epithelium is the characteristic associated with the well-defined border of the avascular PED. A highly reflective IR (upper left panel, open arrow) and hyperautofluorescent lesion (upper central panel, open arrow) disposed in a reticular pattern matches with the reticular area of decreased fluorescence on the late FA (middle right panel, open arrow) and ICGA (bottom right panel, open arrow) frames. The material accumulated in these reticular lesions is responsible for the dense hypereflective deposits seen beneath and within the sensory retina on SD-OCT scan (upper right panel, arrowhead).

to vascularized PED. Only 1/17 of eyes harboring this feature developed. Of note, once a CNV developed in 1 study eye, subretinal fluid at the border of the PED was clearly detected on SD-OCT scan (Fig. 4).

Integrated imaging of avascular serous PED

The dark area of inhomogeneous decreased IR reflectance matched with the area of inhomogeneous increased autofluorescence visualized on FAF, and fluorescence visualized on late FA frames. This area appeared as hypofluorescent on late ICGA frames. SD-OCT scans showed mainly hyporeflective material consistent with serous accumulation of the avascular PED, with some collections of hypereflective material within the PED. The sharp border of increased IR reflectance surrounding the avascular PED matched with the halo of reduced autofluorescence on FAF, and the reduced fluorescence on late FA frames, as well as with the sharp hypofluorescent border on the late ICGA frames. An abrupt elevation of the RPE was seen to be the associated characteristic on SD-OCT (Figs. 1-3).

The highly hyperautofluorescent lesion disposed in a reticular pattern, which showed increased IR reflectance, matched with the reticular area of decreased fluorescence on late FA and ICGA frames. On SD-OCT, the dense hypereflective deposits seen beneath and within the sensory retina correlated with the material accumulated in these reticular lesions, showing IR reflectance and autofluorescence proprieties and masking on FA and ICGA (Figs. 1, 2).

Patient demographics and integrated imaging of vascular PED

Nineteen consecutive treatment-naïve AMD eyes of 19 patients (6 male and 13 female; mean age 78.1 ± 7.4 years, range 65-90 years) with vascular PED who presented in our department over a 1 month period were analyzed regarding cSLO fundus imaging and corresponding high-resolution SD-OCT B-scan features. BCVA ranged from 20/25 to 20/200 (mean 0.43 ± 0.23 LogMAR). In all these eyes, the vascular PED appeared as a dark area of decreased IR reflectance, and as a bright area of increased autofluorescence on FAF frames (Fig. 5). On FA and ICGA, the vascular PED appeared as an area of inhomogeneous increased fluorescence, and as a dark area of inhomogeneous decreased fluorescence, respectively. Of

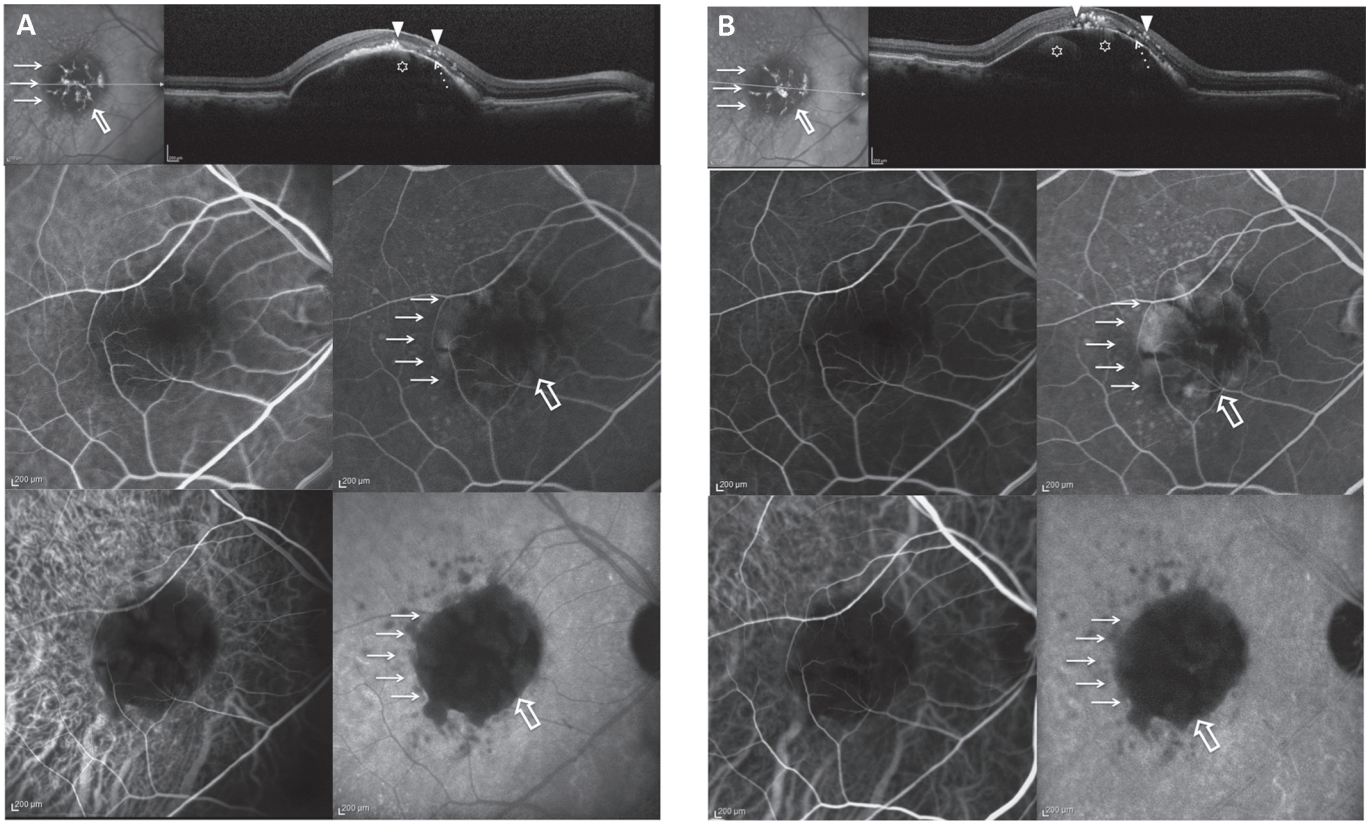

Fig. 3 - Sharp borders of avascular pigment epithelium detachment (PED). Patient 1, right eye, at baseline examination (**A**) and after 24 months (**B**). The infrared (IR) reflectance frame of the fundus (upper left panel) shows the avascular (PED) as a dark area of inhomogeneous decreased IR reflectance surrounded by a sharp border of increased IR reflectance (arrows). Of note, some brighter areas appear on the IR image. The dark area of inhomogeneous decreased IR reflectance matches with the area of inhomogeneous increased fluorescence as visualized on the late fluorescein angiography (FA) frames (middle right panel; the early FA frame is displayed on the middle left panel). This area appears hypofluorescent on the late indocyanine angiography (ICGA) frames (bottom right panel; the early ICGA frame is displayed on the bottom left panel). The sharp border of increased IR reflectance (upper left panel, arrows) surrounding the avascular PED matches with the halo of reduced fluorescence on the late FA frames (bottom left panel, arrows), as well as with the sharp hypofluorescent border on the late ICGA frames (bottom right panel, arrows). Spectral-domain optical coherence tomography (SD-OCT) scan (upper right panel) shows mainly hyporeflective material consistent with serous accumulation of the avascular PED, with some collections of hyperreflective material within the PED (asterisks). On SD-OCT scan, an abrupt elevation of the retinal pigment epithelium is the characteristic associated with the well-defined border of the avascular PED. A highly reflective IR (upper left panel, open arrow) lesion disposed in a reticular pattern matches with the reticular area of decreased fluorescence on the late FA (bottom left panel, open arrow) and ICGA (bottom right panel, open arrow) frames. The material accumulated in these reticular lesions, is responsible for the dense hyperreflective deposits seen beneath and within the sensory retina on SD-OCT scan (upper right panel, arrowheads), associated with the subretinal fluid to some extent (dotted arrow).

note, vascular PED did not show sharp borders on cSLO imaging (IR reflectance, FAF, FA and ICGA), which was different from avascular PED (Fig. 5). Moreover, an increased IR reflectance/autofluorescence disposed in a reticular pattern was clearly detectable in only 2/19 eyes. SD-OCT clearly revealed the presence of subretinal fluid at the border of the vascular PED in all these eyes (Fig. 5).

Discussion

In this study we analyzed a homogeneous series of 23 eyes showing avascular serous PED, which were followed for a mean of 15.5 months. Among the heterogeneous world of AMD, this rare entity was defined here by the absence of an associated neovascular complex on FA and ICGA in at least 2 consecutive follow-up visits. Surprisingly, only 1/23 eyes (4%) developed a CNV during the follow-up at month 12. In the remaining 22/23 eyes, the final diagnosis at the last follow-up visit was still avascular serous PED. The low rate of occurrence of CNV observed here is in contrast to retrospective studies that indicated that the overall risk for developing CNV within 25 months after diagnosis among patients with serous PED associated with AMD is 24%-34% (7-9). The strict selection of our avascular serous PED patients, excluding notching, hot-spot, and hyperfluorescent lesion on ICGA (at least up to 3 months from the diagnosis), may explain this variation.

Our study revealed 3 features constantly observed in avascular serous PED.

First, we constantly observed a reticular pattern, a highly IR reflective and hyperautofluorescent lesion, which matched with the reticular area of decreased (masking effect) fluorescence (on FA and ICGA), suggesting a lipofuscin-like content for

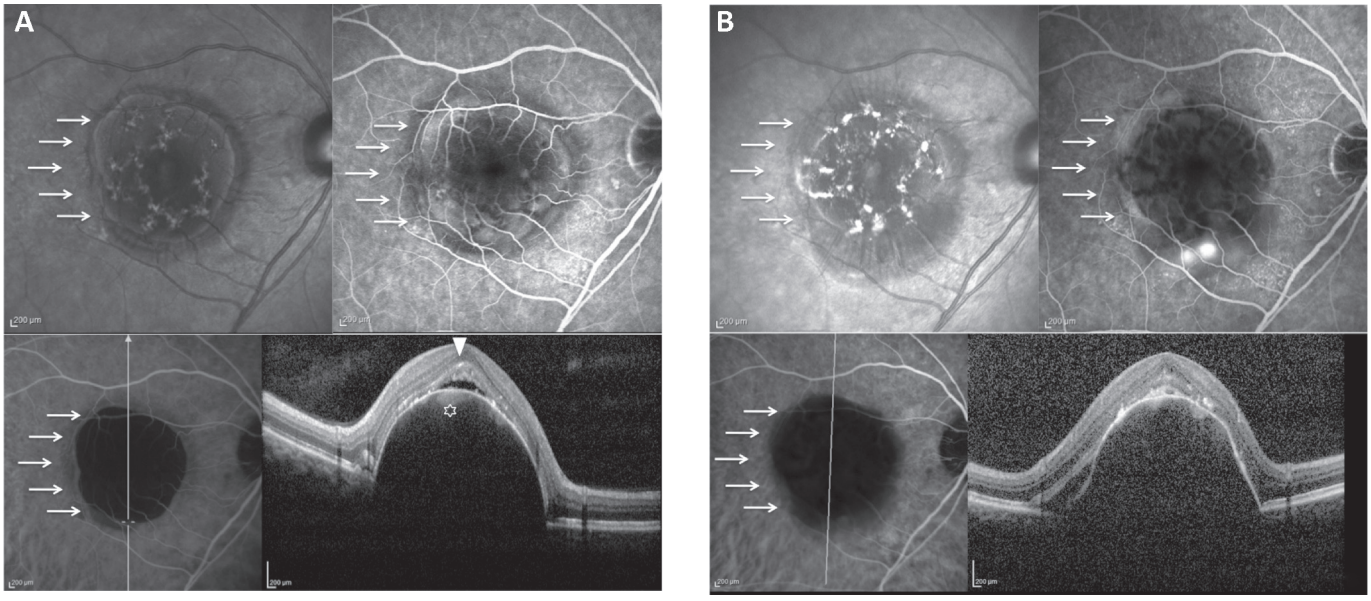

Fig. 4 - Occurrence of choroidal neovascularization (CNV) on avascular pigment epithelium detachment (PED). (**A**) Patient 2, right eye, at baseline. The infrared (IR) reflectance frame of the fundus (upper left panel), showing the avascular PED as a dark area of inhomogeneous decreased IR reflectance, is surrounded by a sharp border of increased IR reflectance (arrows). Note some brighter areas on the IR image. The dark area of inhomogeneous decreased IR reflectance matches with the area of inhomogeneous increased fluorescence as visualized on the late fluorescein angiography (FA) frames (upper right panel). This area appears as hypofluorescent on the late indocyanine angiography (ICGA) frames (bottom left panel). The sharp border of increased IR reflectance (upper left panel, arrows) surrounding the avascular PED matches with the halo of reduced fluorescence on the late FA frames (upper right panel, arrows), as well as with the sharp hypofluorescent border on the late ICGA frames (bottom left panel, arrows). Spectral-domain optical coherence tomography (SD-OCT) scan (bottom right panel) shows mainly hyporeflective material consistent with serous accumulation of the avascular PED, with some collections of hyperreflective material within the PED (asterisk). On SD-OCT scan, an abrupt elevation of the retinal pigment epithelium is the characteristic associated with the well-defined border of the avascular PED. A highly reflective IR (upper left panel, open arrow) lesion disposed in a reticular pattern matches with the reticular area of decreased fluorescence on the late FA (upper right panel, open arrow) and ICGA (bottom left panel, open arrow) frames. The material accumulated in these reticular lesions is responsible for the dense hyperreflective deposits seen beneath and within the sensory retina on SD-OCT scan (upper right panel, arrowhead), which is associated with subretinal hyporeflective fluid under the fovea. (**B**) Patient 2, right eye, 12 months after baseline examination. After the development of CNV, the sharp border of increased infrared (IR) reflectance is no longer detectable (upper left panel, arrows), and the halo of reduced fluorescence on the late fluorescein angiography (FA) frames (upper right panel, arrows) has been replaced by a hyperfluorescent halo. Note the presence of what appear to be radiating choroidal folds. The sharp hypofluorescent border on the late indocyanine green angiography (ICGA) frames (bottom left panel, arrows) appears as a faint hyperfluorescent halo. The SD-OCT scan (bottom right panel) shows subretinal fluid at the site of the CNV.

these lesions. The material accumulated in the reticular lesions, which showed IR reflectance and autofluorescence proprieties, and masking on FA and ICGA, was correlated on SD-OCT with the dense hyperreflective deposits seen beneath and within the sensory retina. Based on the integrated imaging, the lesions here reported in avascular serous PED between the RPE and the inner/outer segment (beneath the sensory retina) appear to be lipofuscin-like, and look very similar to pseudovitelliform lesions in adult-onset foveomacular vitelliform dystsophy (AOFVD) (10, 11). The lipofuscin-like content for the retinal lesion disposed in a reticular pattern (probably derived from the photoreceptors) is compatible with a slow retinal degenerative process associated with avascular PED rather than a sudden and profound intra- and/or subretinal fluid accumulation due to fast growing CNV, as it happens in vascular PED.

Second, subretinal fluid below the fovea was detected in 17/23 eyes (74%, Fig. 1B). This hyporeflective fluid was not associated with progression to vascularized PED in most of the eyes (16/17; Fig. 4A). Thus, we support the assumption that this subretinal fluid below the fovea is not an exudative feature. The association between this hyporeflective fluid and the dense hyperreflective deposits in correspondence with the reticular lesions suggest common mechanisms with the hyporeflective fluid observed in AOFVD.

Third, we observed in all eyes a sharp border of increased IR reflectance surrounding the avascular PED, suggesting the absence of subretinal fluid at the borders of the lesion. In contrast, in the 19 vascularized PED cases, we observed the absence of this sharp border or serous retinal detachment adjacent to the borders. An abrupt elevation of the RPE on SD-OCT scans, without subretinal fluid accumulation, was seen to be the associated characteristic of the sharp border of increased IR reflectance, matching with the halo of reduced autofluorescence on FAF and fluorescence on late FA frames, as well as with the sharp hypofluorescent border on late ICGA frames. Furthermore, SD-OCT scans showed mainly hyporeflective material consistent with serous accumulation of the avascular PED, with some collections of hyperreflective material within the PED, which may contribute to the overall inhomogeneous aspect on IR reflectance, FAF, FA and ICGA.

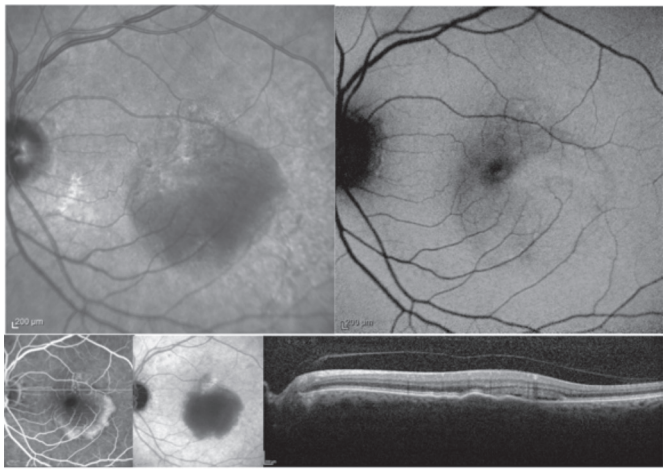

Fig. 5 - Vascularized pigment epithelium detachment (PED). The infrared (IR) reflectance frame of the fundus (upper left panel) shows the vascular PED as a dark area of inhomogeneous decreased IR reflectance. The dark area of inhomogeneous decreased IR reflectance matches with the area of inhomogeneous increased fluorescence as visualized on fundus auto-fluorescence (FAF) (upper right panel) and the late fluorescein angiography (FA) frames (bottom left panel). This area appears as hypofluorescent on the late indocyanine angiography (ICGA) frames (bottom middle panel). No sharp borders appear on the IR reflectance, FAF, FA, and ICGA frames. Spectral-domain optical coherence tomography (SD-OCT) scan (bottom right panel) shows subretinal fluid associated with the choroidal neovascularization.

Pauleikhoff et al (12) proposed that, in the avascular lesions, the fluid would accumulate from the outward movement of ions and material by the RPE (slow accumulation of fluid), while, in vascular lesions, the neovascular complex would contribute to the fluid accumulation (fast accumulation of fluid). They also hypothesized that the hydrophobic barrier in Bruch's membrane may be responsible for the fluid accumulation under the RPE, and that another factor would be responsible for the development of CNV under the RPE ("dual pathogenetic pathway"). Gass (13) hypothesized that PED occurred in AMD from either serous exudation from choriocapillaris hyperpermeability through an intact Bruch's membrane, or by neovascular ingrowth with subsequent exudation from the new vessels directly into the sub-RPE space (ballooning of the RPE monolayer by hydrostatic dissection up above the level of the leaking vessels). Bird and Marshall (14), differently from Gass (13), proposed that the constant deposition of lipid materials into the Bruch's membrane with age renders it increasingly hydrophobic. The increased hydrophobicity and reduced hydraulic conductivity to fluid outflow from the vitreous toward the choroid prompts the accumulation of fluid beneath the RPE. In fact, given that the RPE pumps fluid toward Bruch's membrane, in aged eyes the fluid would accumulate under the RPE monolayer to create a PED instead of passing through the Bruch's membrane. Based on these beliefs, they proposed that CNV was an event that occurred secondary to the PED (14). Similarly, Green et al (15) suggested that CNV might develop as a complication of serous PED.

The main limitations of the current study are the small number of eyes analyzed, as well as the mean follow-up, which was probably too short to study a slowly progressive disease such as avascular serous PED. However, avascular serous PED only accounts for a small percentage of serous PED cases with AMD, and the collection of a large series is not easy (4). Another limit of this study is that we used "last follow-up" as primary endpoint, which, indeed, is not a preferred primary endpoint for case series. Unfortunately, this study was not meant to be a prospective trial. This analysis was only based on our clinical practice, and thus, consecutive patients referred to our department were included, with no prespecified time points.

Our study was not designed to compare avascular serous PED with other subtypes of AMD. Therefore, the specificity of findings, such as the reticular pattern among all other subtypes of AMD, has not been studied. However, our study revealed that the reticular pattern was more commonly observed in avascular serous PED eyes (23/23) than in in vascular PED eyes (2/19; $p<0.05$). Future studies will specifically focus on the ability to use the noninvasive imaging techniques to diagnose an avascular PED, or – at the very least – to support this diagnosis.

We used cSLO ICGA to detect the presence of CNV, and we know that, in some cases, fundus cameras can show hyperfluorescent plaques late in the ICGA that are not apparent using an SLO. Therefore, we admit that among the cases analyzed here, there may be a few with CNV that have been erroneously diagnosed as avascular serous PED. However, the focus was adjusted several times for each image, and several slices were explored in order to try to evidence any hyperfluorescence on late phases of ICG.

In favor of the diagnosis of avascular serous PED, there is the fact that a CNV appeared in only 1 of the 23 studied eyes over a mean follow-up period of 15.5 months. Indeed, we cannot exclude that at least some of our cases may present a form of occult CNV with PED that does not show signs of progression. On the other hand, intravitreal ranibizumab has been performed recently in a series of avascular serous PED (6). None of these cases was improved or stabilized by ranibizumab, suggesting that serous avascular PED is a subgroup distinct from vascularized serous PED.

In conclusion, we describe the integrated imaging of avascular PED in AMD patients, and highlight the peculiar IR, FAF, AF, ICGA, and SD-OCT features. In our series, we constantly observed a reticular aspect, harboring increased IR reflectance, hyperautofluorescence, and hypofluorescent on early phases of FA, which correlated with dense hypereflective deposits seen beneath and within the sensory retina on SD-OCT. In our series, subfoveal hyporeflective fluid did not seem to be correlated with exudative signs of CNV. This report possibly contributes to distinguish avascular serous PED from other clinical identities.

Disclosures

Financial support: No grants or funding have been received for this study.
Conflicts of interest: None of the authors has financial interest related to this study to disclose

References

1. Bressler NM. Age-related macular degeneration is the leading cause of blindness. JAMA. 2004;291(15):1900-1901.

2. Klein R, Klein BE, Jensen SC, Meuer SM. The five-year incidence and progression of age-related maculopathy: the Beaver Dam Eye Study. Ophthalmology. 1997;104(1):7-21.
3. Zayit-Soudry S, Moroz I, Loewenstein A. Retinal pigment epithelial detachment. Surv Ophthalmol. 2007;52(3):227-243.
4. Yannuzzi LA, Slakter JS, Sorenson JA, Guyer DR, Orlock DA. Digital indocyanine green videoangiography and choroidal neovascularization. Retina. 1992;12(3):191-223.
5. Yannuzzi LA, Hope-Ross M, Slakter JS, et al. Analysis of vascularized pigment epithelial detachments using indocyanine green videoangiography. Retina. 1994;14(2):99-113.
6. Ritter M, Bolz M, Sacu S, et al. Effect of intravitreal ranibizumab in avascular pigment epithelial detachment. Eye (Lond). 2010;24(6):962-968.
7. Elman MJ, Fine SL, Murphy RP, Patz A, Auer C. The natural history of serous retinal pigment epithelium detachment in patients with age-related macular degeneration. Ophthalmology. 1986;93(2):224-230.
8. Hartnett ME, Weiter JJ, Garsd A, Jalkh AE. Classification of retinal pigment epithelial detachments associated with drusen. Graefes Arch Clin Exp Ophthalmol. 1992;230(1): 11-19.
9. Shiraki K, Kohno T, Ataka S, Abe K, Inoue K, Miki T. Thinning and small holes at an impending tear of a retinal pigment epithelial detachment. Graefes Arch Clin Exp Ophthalmol. 2001; 239(6):430-436.
10. Puche N, Querques G, Benhamou N, et al. High-resolution spectral domain optical coherence tomography features in adult onset foveomacular vitelliform dystrophy. Br J Ophthalmol. 2010;94(9):1190-1196.
11. Benhamou N, Souied EH, Zolf R, Coscas F, Coscas G, Soubrane G. Adult-onset foveomacular vitelliform dystrophy: a study by optical coherence tomography. Am J Ophthalmol. 2003;135(3):362-367.
12. Pauleikhoff D, Löffert D, Spital G, et al. Pigment epithelial detachment in the elderly. Clinical differentiation, natural course and pathogenetic implications. Graefes Arch Clin Exp Ophthalmol. 2002;240(7):533-538.
13. Gass JD. Drusen and disciform macular detachment and degeneration. Trans Am Ophthalmol Soc. 1972;70:409-436.
14. Bird AC, Marshall J. Retinal pigment epithelial detachments in the elderly. Trans Ophthalmol Soc U K. 1986;105(Pt 6):674-682.
15. Green WR, McDonnell PJ, Yeo JH. Pathologic features of senile macular degeneration. Ophthalmology. 1985;92(5):615-627.